JOURNAL OF MATERIALS SCIENCE **40** (2005) 3367–3373

Manifestation of Nd ions on the structure, Raman and IR spectra of (TeO_2-MoO-Nd_2O_3) glasses

I. SHALTOUT
Physics Department, Faculty of Science, Al Azhar University, Nasr City 18841, Cairo, Egypt
Y. BADR*
National Institute of Laser Enhancement Sciences (NILES), Cairo University, Egypt
E-mail: ybadr@hotmail.com

The structure of [80TeO_2 + (20–x)MoO + xNd_2O_3] glasses, with $x = 0$, 4, 6, 10 and 12 mol%, is studied in this work. Raman scattering in the spectral range (−2000 to 3500 cm^{-1}) and IR absorption spectra have been measured for crystalline TeO_2 and glasses, and their assignments were discussed and compared. Many vibrational modes were found active in both Raman and IR and their assignments for crystalline TeO_2 and for the glasses were discussed in relation to the tetragonal structure of crystalline α-TeO_2. Nd_2O_3 was found to completely eliminate diffuse scattering and enhance the Raman scattering intensity. Anti-stokes Raman bands in the range −1460 cm^{-1} to −1975 cm^{-1} were observed for both (30Li_2O + 70B_2O_3 + xNd_2O_3) glasses and [80TeO_2 + (20 − x)MoO + xNd_2O_3] glasses and were attributed to some emission processes due to the doping of the glasses with Nd_2O_3.

1. Introduction

Due to their stability, low crystallization rate, excellent transparency in a wide spectral region (3–18 μm) and many other significant properties, Tellurite glasses are important in many technological applications. As reported in the literature, TeO_2 based glasses are considered as excellent materials for possible uses in nonlinear optical devices, host materials for upconversion fluorescence of rare earth ions and high speed laser communication systems [1, 2]. Such importance of Tellurite glasses is in principle due to their specifically high electron-phonon anharmonicity [3]. The structure of binary (TeO_2-MoO) glasses and (TeO_2-MoO) crystalline systems and some other TeO_2-based glasses have been studied by XRD analysis, IR, Raman scattering and DSC [4–10], where bond lengths, way of bonding and the interactions among TeO_4, TeO_{3+1}, TeO_3 and the glass modifier cations have been discussed.

TeO_2-based glasses are known as good hosts for rare earth ions (e.g. Nd^{2+}, Er^{3+}) in possible uses for practical laser applications [11]. Upconversion fluorescence was observed for the first time in Tellurite glasses of the composition (70TeO_2·30Na_2O·1Er_2O_3), and Er^{3+} ions were found to be relatively more important in Tellurite glasses than Nd^{2+} [12, 13]. Some important properties of Er^{3+} doped Tellurite glass fibers have been published and this work has attracted a strong attention because of its importance in increasing the transmission capacity of some high-speed communication systems [14, 15]. Upconversion fluorescence has been reported in several Tellurite glasses doped with Ho^{3+} and these glasses were expected to be used as upconversion laser materials [16].

Tellurite glasses containing GaO_2 are known as promising glasses of high thermal stability and chemical resistance and could be used in improving the fiber amplifier efficiency [17]. Glasses of the system (ZnF_2-PbO-TeO_2) show a high transparency in the 3 to 18 μm region and they are considered as best materials for uses as optical components, filters, and laser windows [18]. Optical absorption and photoluminescence properties of Eu^{3+}-doped (TeO_2-ZnF_2-PbO) glasses have been studied and different possible laser emission transitions were discussed [18–21].

Glasses of the composition [80TeO_2-10Nb_2O_5-5Li_2O-5K_2O] doped with 0.5–10 mol% of Nd_2O_3 have been studied by Raman scattering, DSC and were found to be more thermally stable as Nd_2O_3 increases and this was attributed to an increase in the rigidity of the glasses with the addition of Nd_2O_3 [22]. These glasses were suggested to be utilized as rare earth containing amplifying devices, where its emission cross-sections were reported to be the largest among oxide glasses. In the present work we study the effect of Nd_2O_3 on the structure of [80TeO_2 + (20 − x)MoO + xNd_2O_3] glasses, with $x = 0$, 4, 6, 10 and 12 mol% using FIR to MIR absorption in the range (80 cm^{-1} to 4000 cm^{-1}) and Raman scattering in the spectral range (−2000 cm^{-1} to 3500 cm^{-1}). The negative sign before the frequency values placed here and for the

*Author to whom all correspondence should be addressed.

Raman spectra hereinafter means negative frequency shift.

2. Experimental

Glass samples of the composition $[80TeO_2 + (20 - x)MoO + xNd_2O_3]$, with $x = 0$, 4, 6, 10 and 12 mol% have been prepared by fusing the respective proportions of the reagent grade oxides (TeO_2, MoO and Nd_2O_3 Aldrich chemicals 99.995%) in a platinum crucible in a preheated furnace at 800°C for about 30 min. After complete fusion, the melt was poured on a stainless steel plate at room temperature and quickly pressed by a similar plate. Bulk samples of ∼2 cm diameter and ∼0.5 mm thickness were obtained. Samples have not been subjected to any annealing process and its glassy state was confirmed using X-ray diffraction XRD. Glass samples are labeled in the present work as TNd0G, TNd4G, TNd6G, TNd10G and TNd12G, respectively for $x = 0$, 4, 6, 10 and 12 mol%. The glass formation range GFR of the present system was found to contain up to 12 mol% of Nd_2O_3, and no glasses was obtained beyond this limit.

The FT-Raman and IR spectra were measured at room temperature for the as casting samples using BRUKER FT-Raman spectrometer of type RFS 100/S, which is attached to BRUKER-IFS 66/S spectrometer. The RFS 100/S version provides flexible sample handling and optimum FT-Raman performance. This system is equipped with a broad-range Quartz beam splitter; BRUKER's patented frictionless interferometer with its ROCKSOLID alignment provides high sensitivity and stability. The diode-pumped, air-cooled Nd-YAG laser source with maximum laser power of 1500 mW is controlled completely through software. The standard RFS 100/S configuration provides a spectral range of 70–3600 cm^{-1} (stokes' shift), and -100 to -2000 cm^{-1} (anti-stokes shift). Raman spectra of (as casting) bulk glass samples of the present work have been measured with a resolution of 2 cm^{-1} using 1064 nm laser line with a power of 100 mW over the whole spectral range. The high precession air bearing interferometer provides high resolution to better than 0.1 cm^{-1}. However, it was found that a resolution of 2 cm^{-1} is appropriate for glasses of the present work. IR spectra in the range 400 cm^{-1} to 4000 cm^{-1} have been collected for powder glass samples dispersed in spec-pure KBr pallets with a resolution of 2 cm^{-1} and a laser power of 100 mW at room temperature. FIR spectrum of crystalline TeO_2 in the range (80–400 cm^{-1}) has been collected by dispersing its powder in low-density polyethylene.

3. Results and discussions

Fig. 1 shows the Raman spectrum of crystalline TeO_2 in the spectral range (-2000 cm^{-1} to $+3500$ cm^{-1}). As seen in the figure four strong Stokes' Raman bands are observed at 122, 149, 392 and 646 cm^{-1}. These bands are also observed as antisokes' bands with much lower relative intensities respectively at -122, -148, -391 and -646 cm^{-1}. Figs 2a and b shows a comparison of the Raman spectrum from 0–1000 cm^{-1} and the

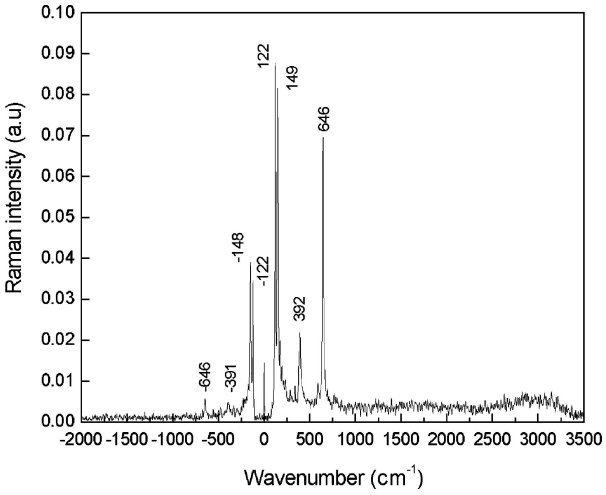

Figure 1 Raman spectrum of crystalline TeO_2.

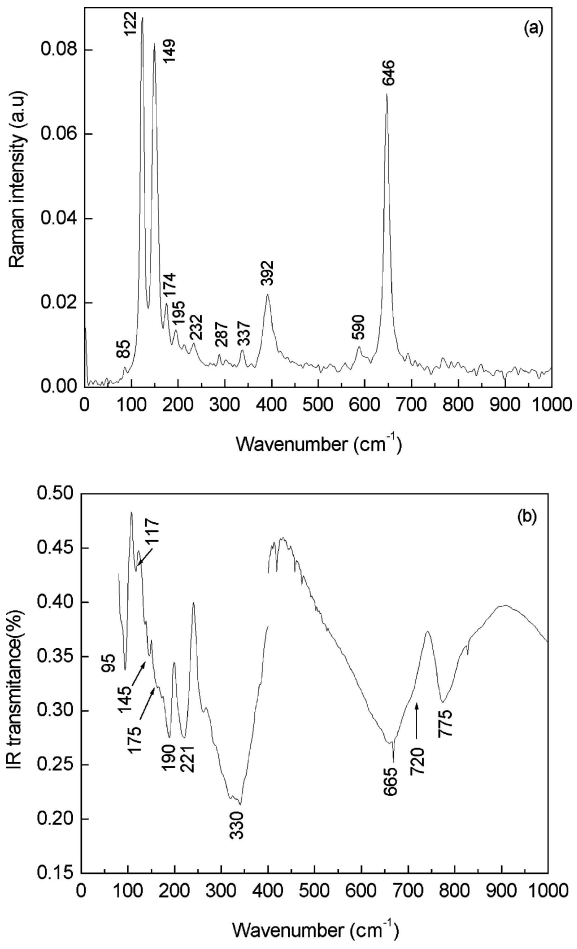

Figure 2 A blow up of the Raman spectrum of crystalline TeO_2 (a), FIR-MIR spectra of crystalline TeO_2 (b).

IR spectrum in the range 80–1000 cm^{-1} of crystalline TeO_2. Crystalline TeO_2 has two well known crystalline structures; α-TeO_2 of [D_{4h}^{14} (rutile), D_4^4 and D_4^8 (paratellurite)] space groups] and β-TeO_2 (Tellurite) [6, 7, 10, 23, 24]. The two α-TeO_2 tetragonal structures with D_{4h}^{14} symmetry (rutile) or D_4^4, D_4^8 symmetry (paratellurite) have four vibrational modes active in both Raman and IR and assigned to the vibrational modes of the triagonal bipyramids tbps TeO_4 tetrahedral units [2, 18–21]. In both structures, (rutile, paratellurite) the structural units are triagonal bipyramids tbps with two oxygen

atoms in the equatorial position and two oxygen atoms in the axial position. The tbps are deformed, where the Te atom is not at the center of the equatorial plane and the third position in this plane is occupied with a free electron pair. δ-TeO_2 crystalline phase, and γ-TeO_2 orthorhombic metastable crystalline phase are known as well [23–26]. The relatively new δ-TeO_2 and γ-TeO_2 crystalline phases have been investigated in studying the crystallization process of some TeO_2-glasses [23]. γ-TeO_2 crystalline phase was considered the most possible short range order structure for TeO_2 glasses due to its direct formation during heating of the glasses, the good correspondence of the Raman spectrum and the TeO_2-glass with that of the γ-TeO_2 crystalline phase, and finally due to the best correspondence of the calculated vibrational state density distribution VSDD of the γ-TeO_2 phase and the TeO_2-glass [23].

On the other hand, it has been well established that the TeO_2-glass structure is composed of TeO_4 triagonal bipyramids (tbps) connected by vertices as the α-TeO_2 crystalline phase and that the increase of the modifier content converts these TeO_4 tetrahedra to TeO_{3+1} polyhedra and TeO_3 units [22, 27–29].

The Raman spectrum of crystalline TeO_2 measured in the present work, Fig. 1, is characteristic of α-TeO_2 [22, 23] and could be assigned to the vibrational modes of the triagonal bipyramids tbps of the TeO_4 tetragonal units. The band at 392 cm^{-1} is due to the axial bending vibrational mode $(O_{ax}{-}T{-}O_{ax})_b$ and the band at 646 cm^{-1} is due to the axial symmetric stretching vibrational mode $(Te_{ax}{-}O)_s$ of the TeO_4 tetrahedra [18–21]. In Fig. 2b the IR band at 665 cm^{-1} is corresponding to the Raman band at 646 cm^{-1} attributed to the axial symmetric stretching vibrational mode $(Te_{ax}{-}O)_s$, Fig. 2a. The IR shoulder at ~720 cm^{-1} and the resolved band at 775 cm^{-1} observed in the MIR spectrum of crystalline TeO_2 are due to the equatorial symmetric stretching $(Te_{eq}{-}O)_s$ and the equatorial antisymmetric stretching $(Te_{eq}{-}O)_{as}$ vibrational modes [2, 18–21]. The strongest IR band of crystalline TeO_2 centered at 330 cm^{-1} is observed relatively weak in the Raman spectrum at 337 cm^{-1}, and the sharp IR peaks at 95, 190, and 221 cm^{-1} are observed relatively weak in the Raman spectrum around the same positions as seen in Fig. 2. The dominant very strong Raman bands at 122, 149 cm^{-1} are observed as unresolved shoulders in the IR spectrum at ~117 and ~145 cm^{-1}. The activity of these vibrational modes of crystalline TeO_2 in both Raman and IR as seen here is characteristic of crystalline α-TeO_2 [17, 18, 21, 23]. The small frequency differences between the bands observed in both Raman and IR spectra could be due to the fact that Raman scattering spectra were measured on as-casting bulk glass samples while the IR spectra have been collected from powder glass samples dispersed in KBr pallets.

Raman spectra of glasses are shown in Fig. 3. As seen in this figure, no Raman bands could be observed for the TNd0G glass sample (free of Nd_2O_3) due to the strong diffuse scattering around 3150 cm^{-1}. Fig. 4a shows this diffuse scattering observed for this glass sample measured with different laser power values ranging from 100 mW to 550 mW. A laser power of 100 mW could

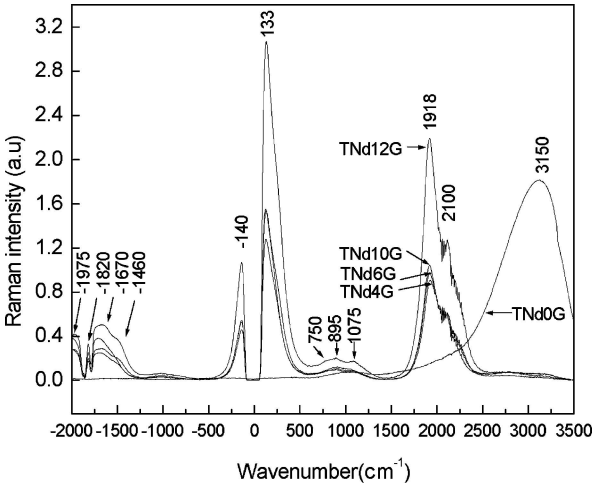

Figure 3 Raman spectra of the $[80TeO_2 + (20 - x)MoO + xNd_2O_3]$ glasses, with $x = 0$, 4, 6, 10 and 12 mole%.

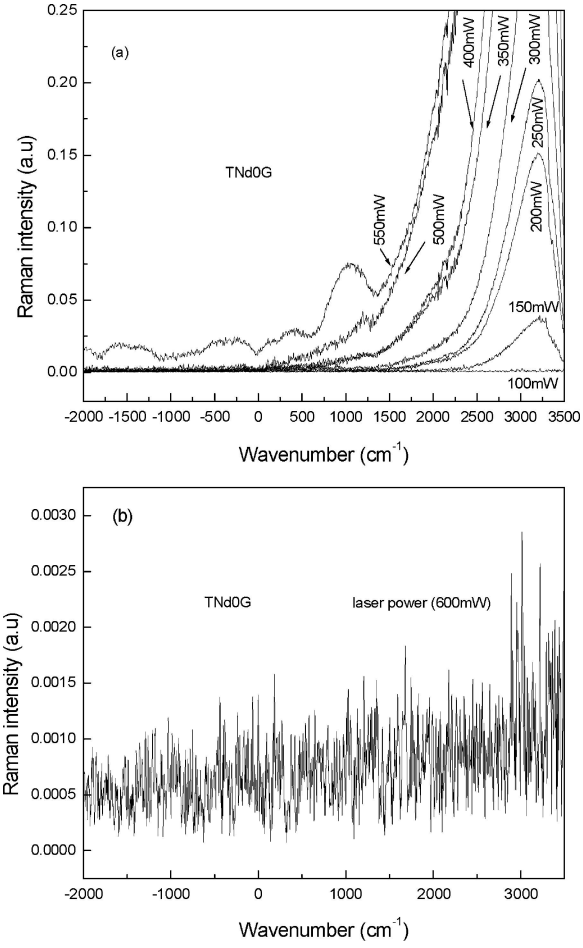

Figure 4 Raman spectra for the TNd0G glass, excited with different laser power values (a), with a laser power of 600 mW, (b).

not excite the Raman spectrum for this sample as shown in Fig. 4a. The very strong diffuse scattering around 3150 cm^{-1} which increases with the laser power from 150 mW to 550 mW, Fig. 4a, made it hard to detect the Raman bands for this sample. Only with a laser power of 550 mW, a few Raman bands started to be observable between -2000 cm^{-1} and $+1500$ cm^{-1}. We tried to overcome diffuse scattering by increasing the laser power to 600 mW. However, diffuse scattering dominated the whole range and no spectrum could

be observed at all as seen in Fig. 4b. It seems that the thermal effect of the high power laser (600 mW) shining the sample may have ruptured the glass structure and resulted in no photon scattering. Raman spectra for other glass compositions (TNd4G, TNd6G, TNd10G, TNd12G), shown in Fig. 3, were easily collected with a laser power of 100 mW.

The Raman spectra of the glasses doped with Nd_2O_3 (TNd4G, TNd6G, TNd10G, TNd12G) show very strong Raman bands at 2100, 1918, 133, −140, −1460, −1670, −1820 and −1975 cm^{-1} as shown in Fig. 3. These bands are not observed for crystalline TeO_2 as shown in Fig. 1. It is clear from Fig. 3 that the addition of Nd_2O_3 enhanced the Raman intensities of all bands and completely eliminated the diffuse scattering shown by the TNd0G glass sample. The Raman intensities of all bands are increasing as Nd_2O_3 content increases and show maximum values for the sample containing the highest content of Nd_2O_3 as shown in Fig. 3. The broad band centered at 133 cm^{-1} seen in Fig. 3 may represent an overlap of the stokes' Raman bands of crystalline TeO_2 at (122, 149 cm^{-1}) seen in Fig. 1. Similarly, the anti-stokes band of the glass samples at –140 cm^{-1} is an overlap of the two anti-stokes bands of crystalline TeO_2 at (−122, −148 cm^{-1}). These two bands represent the most intense vibrations of crystalline TeO_2 and its strong appearance in all glass samples suggests that the short-range order SRO of these glasses is a disordered version of crystalline α-TeO_2. The broadening and the asymmetry of the Raman bands of the glasses at +133 cm^{-1} and −140 cm^{-1} are due to its disordered nature, where acoustic Raman AR bands arising from the disordered nature could be embedded under the these strong peaks. AR bands at frequencies of ∼40 to100 cm^{-1} known as Boson peaks, associated to light scattering due to acoustic-like vibrations of the disordered structure, have been seen in many oxide glasses including Tellurites and its origin still a matter of debate [27, 30–34]. These AR peaks are usually seen overlapped with some Raman modes of vibrations of the glass matrix, that is, vibrational modes of the basic structural units of the glass former and the glass modifier cations. A low frequency band at ∼130 cm^{-1} has been observed in a previous work on (GeO_2-TeO_2-PbO-CaO) glasses and was assigned to the modifier-nonbridging oxygens NBO vibrations of the (Pb─O) bonds [27].

On comparison of Figs 2a and 3, it is interesting to notice that the relatively weak features in the range 174–337 cm^{-1} and the very strong bands at 392, 646cm^{-1} characteristics of TeO_4 tbps of crystalline α-TeO_2, Fig. 2a, have been disappeared in the spectra of the glasses. That is, Nd_2O_3 is strongly affecting the short-range order SRO structure of the present glasses. In Fig. 3, the weak broad band centered around 750 cm^{-1} observed for all glasses containing Nd_2O_3 could be an envelope assigned to the $(Te_{eq}─O)_s$ and the $(Te_{eq}─O)_{as}$ vibrational modes of some amount of TeO_{3+1} polyhedra and/or TeO_3 triagonal pyramids tps formed in the glasses of the present work [2, 18–21]. A Raman band in the range 420–450 cm^{-1} have been observed in a previous work for many TeO_2-glasses and was assigned to the symmetric stretching and bending vibrations of (Te─O─Te) linkages which are formed by vertex-sharing of (TeO_4), (TeO_{3+1}) polyhedra and (TeO_3) units [27, 29]. However, this band does not appear in the spectra of the present work and could be embedded underneath the very intense dominant Raman peak at 133 cm^{-1}. Such apparent discrepancies may be due to the fact that some modes could be caused by anharmonic combinations of frequencies, which are typical for Tellurite glasses [35].

Two other broad bands with low relative intensities are observed in the Raman spectra of the glasses in Fig. 3 at ∼895, ∼1075 cm^{-1}. These two bands could be assigned respectively to the stretching vibrations of (Mo═O) bonds of deformed MoO_6 octahedra and to the vibrations of (Mo─ O─ Mo) bridging bonds [28]. The strong band at 1918 cm^{-1} and the shoulder centered around 2100 cm^{-1} observed for all glasses have no specific assignments and need to be more clarified and discussed.

Figs 5a and b shows the Raman intensity and the bandwidth at half maximum BWHM of the Raman bands as a function of Nd_2O_3. As shown, the Raman intensity of almost all bands shows maximum

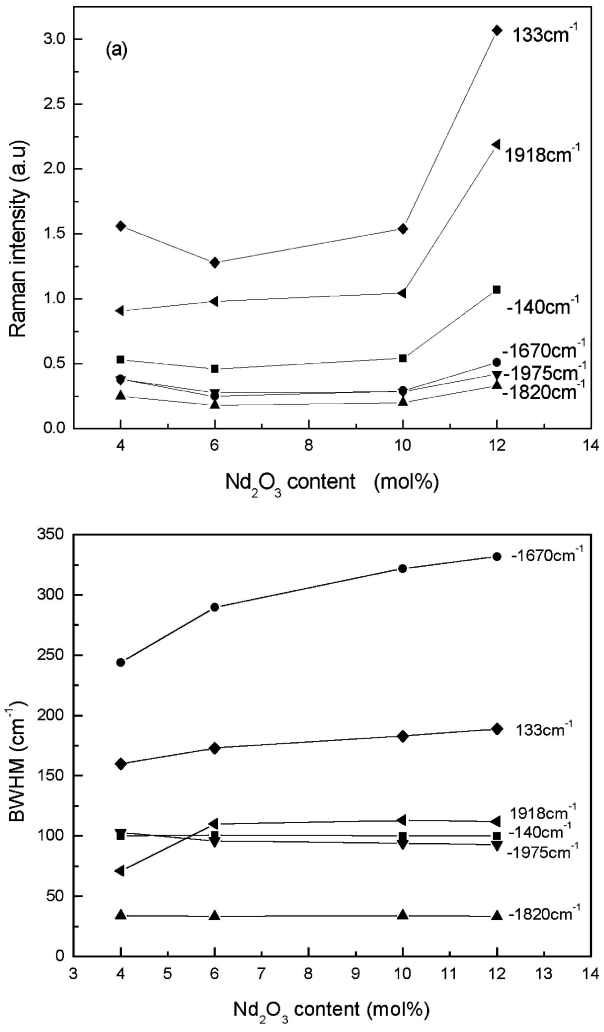

Figure 5 Raman intensity (a), BWHM (b) as a function of Nd_2O_3 content for the $[80TeO_2 + (20 - x)MoO + xNd_2O_3]$ glasses.

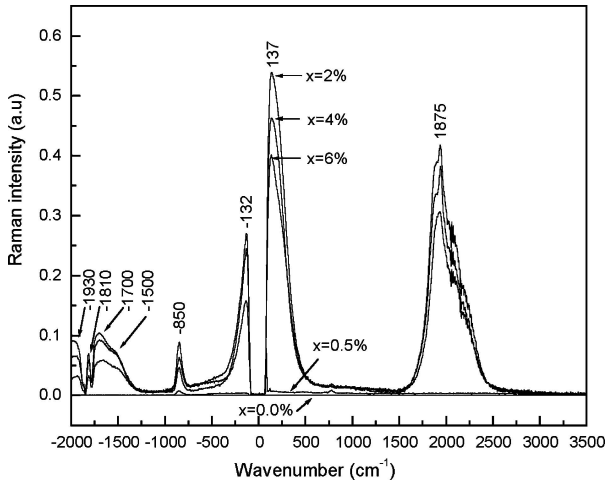

Figure 6 Raman spectra of ($30Li_2O + 70B_2O_3 + xNd_2O_3$) glasses, with $x = 0$, 0.5, 2, 4 and 6 mole%.

values for the sample with the highest content of Nd_2O_3 (TNd12G). Also, the BWHM of the bands at -1670 cm^{-1}, 133 cm^{-1} and at 1918 cm^{-1} are increasing as Nd_2O_3 increases. This dependence of the Raman intensity and the BWHM on Nd_2O_3 content shows the strong effect of Nd_2O_3 on the structure of the glasses.

To show the effect of Nd_2O_3 on the Raman scattering from a different oxide glass system, we present the Raman spectra of ($30Li_2O + 70B_2O_3 + xNd_2O_3$) glasses, with $0 \leq x \leq 6$ mole%, measured in a previous work and shown in Fig. 6 [36], to be compared with the Raman spectra of $[80TeO_2 + (20-x)MoO + xNd_2O_3]$ glasses of the present work. As shown in Fig. 6, for the glass sample free of Nd_2O_3 ($x = 0$) no Raman bands are observed at all, and for the glass sample with $x = 0.5$ mole% some very weak bands are hardly seen. Glasses with $x = 2$, 4 and 6 mole% of Nd_2O_3 show strong stokes' bands at 137 and 1875 cm^{-1}. The relative intensities and frequency positions of these two bands are very close to the bands at 133 and 1918 cm^{-1} of the $[80TeO_2 + (20-x)MoO + xNd_2O_3]$ glasses shown in Fig. 3. The anti-stokes bands observed at (-1500, -1700, -1810 and -1930 cm^{-1}) for ($30Li_2O + 70B_2O_3 + xNd_2O_3$) glasses with $x = 2$ to 6 mol% are very similar to those of the ($TeO_2 + MoO + Nd_2O_3$) glasses seen in Fig. 3. The closed correspondence of frequency positions and relative intensities of these Raman bands in two completely different glassy materials manifests the strong effect of Nd_2O_3 on the structure of these glasses.

Figs 7a and b show a comparison of the anti-stokes Raman bands of the $[80TeO_2 + (20 - x)MoO + xNd_2O_3]$ glasses and ($30Li_2O$-$70B_2O_3$ – xNd_2O_3) glasses. The relative intensities, positions and the closed similarity of the anti-stokes bands in these completely different glass matrices suggest that these bands are due to some emission processes due to Nd^{++} ions. Further Raman and optical absorption measurements on [(Li_2O-B_2O_3-Nd_2O_3), (TeO_2-MoO-Nd_2O_3)] glasses and its dependence on composition and temperature are being now under consideration to get quantitative information about any possible emission processes due to Nd_2O_3.

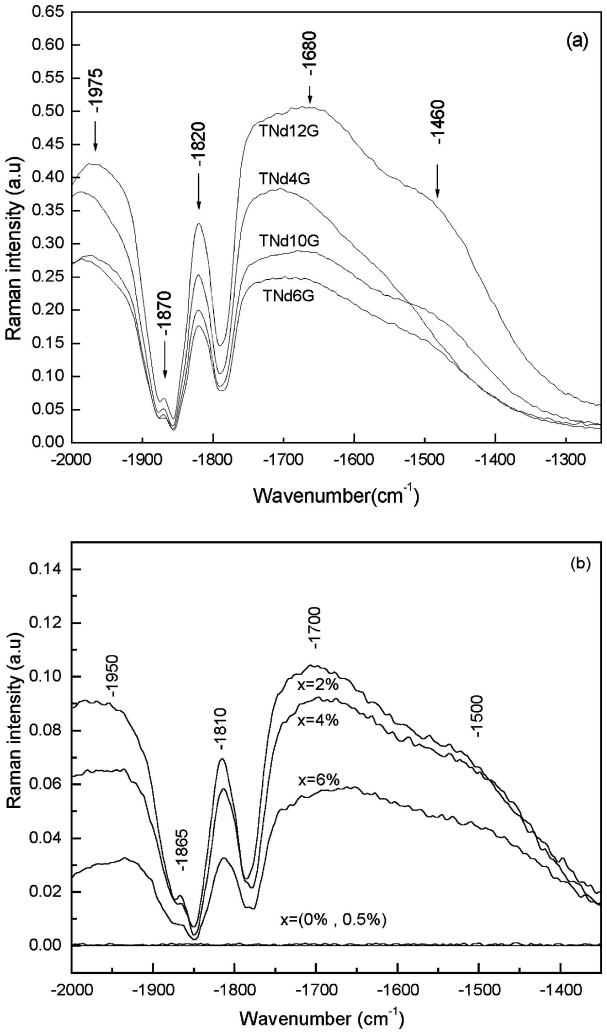

Figure 7 Enlarged anti-stokes Raman spectra of the $[80TeO_2 + (20 - x)MoO + xNd_2O_3]$ glasses (a), and the $[30Li_2O + 70B_2O_3 + xNd_2O_3]$ glasses (b).

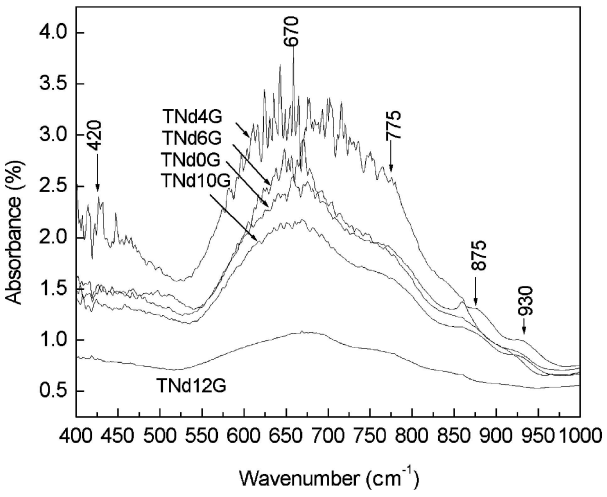

Figure 8 MIR spectra of the $[80TeO_2 + (20 - x)MoO + xNd_2O_3]$ glasses, with $x = 0$, 4, 6, 10 and 12 mole%.

Fig. 8 shows the IR absorption spectra of the glasses. The main band at ~670 cm^{-1} is due to the axial symmetric stretching vibrational modes $(Te_{ax}{-}O)_s$ of TeO_4 tetrahedra [2, 18–21]. This band is corresponding to the IR band at 665 cm^{-1} and to the Raman band at 646 cm^{-1}of crystalline TeO_2 observed in Figs 2a and b. The unresolved IR shoulder at ~750

to ~775 cm^{-1} observed for all glasses could be an envelope corresponding to the equatorial symmetric vibrations $(Te_{eq}—O)_s$ and the equatorial asymmetric vibrations $(Te_{eq}—O)_{as}$ observed in the Raman spectra of the glasses shown in Fig. 3. The IR broad band centered at ~420 cm^{-1} for all glasses has been observed in some previous work on tellurite glasses and was assigned to the (glass former–glass modifier) bridging bonds [28, 30]. For the glasses of the present work, it could be assigned to the (Te—O—Mo) and/or (Te—O—Nd) stretching vibrations where the modifier cations (Mo and/or Nd) may incorporate in the glass matrix by bonding with TeO_4 tetrahedra through Oxygens.

Two other bands with low relative intensities are observed in the IR spectra of the glasses in Fig. 8 as shoulders at ~875 and ~930 cm^{-1}. These two bands could be assigned respectively to the stretching vibrations of (Mo=O) bonds of the deformed MoO_6 octahedra and to the vibrations of (Mo—O—Mo) bridging bonds [28]. Crystalline MoO consists of deformed MoO_6 octahedra and is known to have a strong IR band at 985 cm^{-1} and two bands at ~870 cm^{-1} and 813 cm^{-1} [29]. An IR band at ~910 cm^{-1} has been previously observed in a binary TeO_2—MoO glasses and was assigned to Mo—O non-bridging stretching modes [28].

4. Conclusions

The Glass formation range of $[80TeO_2 + (20 - x)MoO + xNd_2O_3]$ glasses, with $x = 0,4,6,10$ and 12 mol%, was found to contain an upper limit of 12 mol% of Nd_2O_3. The effect of Nd_2O_3 on the structure of these glasses has been studied in this work using Raman scattering and IR spectroscopy. The axial symmetric stretching vibrations $(Te_{ax}—O)_s$, the equatorial symmetric vibrations $(Te_{eq}—O)_s$ and the equatorial antisymmetric vibrations $(Te_{eq}—O)_{as}$ have been observed for crystalline TeO_2 in both Raman and IR. Assignments of the Raman and the IR spectra of crystalline TeO_2 have been compared and were found characteristics of α-TeO_2. The presence, positions and intensities of many vibrational modes in both Raman and IR spectra of the glasses and the possible roles of Nd_2O_3 and MoO have been discussed in relation to the tetragonal structure of crystalline α-TeO_2 with D_{4h}^{14} symmetry (rutile) or D_4^4 symmetry (paratellurite). It was found that, the addition of Nd_2O_3 very much enhances the Raman intensities and completely eliminates the diffuse scattering shown by the Nd_2O_3 free sample. The relative intensities and the BWHM of the Raman stokes' bands at 133 cm^{-1}, 1918 cm^{-1} and of the anti-stokes bands at -140 cm^{-1}, -1670 cm^{-1}, -1820 cm^{-1}, -1975 cm^{-1} of the glasses were found dependent on Nd_2O_3 content with maximum values for the sample with the highest content of Nd_2O_3. The anti-stokes Raman bands of $(30Li_2O + 70B_2O_3 + xNd_2O_3)$ glasses and $[80TeO_2 + (20 - x)MoO + xNd_2O_3]$ glasses have been compared. It has been suggested that these bands are strongly related to Nd_2O_3 and are attributed to some emission processes of Nd^{++} ions. Further Raman and optical absorption measurements and quantitative analysis will be considered in a future work on these glass systems.

References

1. H. NASU, O. MATSUSHITA, K. KAMIYA and H. KUBODERA, *J. Non. Cryst. Solids* **124** (1990) 275.
2. S. H. KIM, T. YOKA and S. SAKA, *J. Amer. Ceram. Soc.* **76** (1993) 865.
3. I. V. KITYK, J. KASPERCZYK and K. PLUCINSKI, *J. Opt. Soc. America B V16* **10** (1999) 1719.
4. H. HIROSHI, I. MICHIHISA and T. YOSHIDA, *J. Non. Cryst. Solids* **86** (1986) 327.
5. E. F. LAMBSON, G. A. SANDERS, B. BRIDGE and R. A. ELMALLAWANY, *J. Non. Cryst. Solids* **69** (1984) 117.
6. S. NEOV, E. GREVASSIMOVA and B. SYDZHIMOV, *Phys. Status Solidi (a)* **76** (1983) 297.
7. Y. DIMITRRIEV, V. DIMITROV and M. ARANUDOV, *J. Mat. Sci.* **18** (1983) 1353.
8. I. SHALTOUT, YI TANG, R. BRAUNSTEIN and A. M. ABU EL-AZM, *J. Phys. Chem. Solids* **56** (1995) 141.
9. I. SHALTOUT, YI TANG, R. BRAUNSTEIN and E. E. SHAISHA, *J. Phys. Chem. Solids* **57** (1996) 1223.
10. I. SHALTOUT, *J. Mat. Sci.* **35** (2000) 323.
11. M. J. WEBER, J. D. MYERS and D. H. BLACKBURN, *J. Appl. Phys.* **52** (1981) 2944.
12. S. TANABE, K. HIRAO and N. SOGA, *J. Non. Cryst. Solids* **122** (1990) 79.
13. H. NII, K. OZAKI, M. HERREN and M. MORITA, *J. Lumin.* **76/77** (1998) 116.
14. A. MORI, Y. OHISHI and S. SUDO, *Electron. Lett* **33** (1997) 863.
15. L. L. NEINDRE, SHIBIN JIANG, BOR-CHYUAN HWANG, TABLUO and JASON WATSON, *J. Non. Cryst. Solids* **255** (1999) 97.
16. K. HIRAO, S. KOSHIMOTO, K. TANAKA, S. TANABE and N. SOGA, *J. Non. Cryst. Solids.* **139** (1992) 151.
17. J. RULLER and J. SHELBY, *J. Phys. Chem. Solids* **33** (1992) 177.
18. V. RAVI KUMAR and N. VEERAIAH, *J. Phys. Chem. Solids* **59** (1998) 91.
19. V. RAVI KUMAR, N. VEERAIAH, B. APPA RAO and S. BHUDDUDU, *J. Mat. Sci.* **33** (1998) 2659.
20. G. AMARNATH, S. BUDDHUDU and F. G. BRAYANT, *J. Lumin.* **15** (1991) 17.
21. G. AMARNATH, S. BUDDHUDU and F. G. BRAYANT, *J. Non. Cryst. Solids* **122** (1990) 86.
22. FABIA C. CASSANJES, YOUNES MESSADDEQ, LUIZ F. C. DE OLIVEIRA, LILIA C. COURROL, LAERCIO GOMES and SIDNEY J. L. RIBEIRO, *J. Non. Cryst. Solids* **1247** (1999) 58.
23. O. NOGUERA, T. MERLE-MEJEAN, A. P. MIRGORODSKY, M. B. SMIRNOV, P. THOMAS and J. C. CHAMPARNAUD-MESJARD, *J. Non. Cryst. Solids* **330** (2003) 50.
24. R. A. F. EL-MALLAWANY, "Tellurite Glasses Handbook: Properties and Data, CRC," Boca Raton, FL, 2002.
25. S. BLANCHANDIN, P. MARCHET, P. THOMAS, J. C. CHAMPARNAUD-MESJARD, B. FRIT and A. CHAGRAOUI, *J. Mat. Sci.* **34** (1999) 4285.
26. J. C. CHAMPARNAUD-MESJARD, S. BLANCHANDIN, P. THOMAS, A. MIRGORODSKY, T. MERLE-MEJEAN and B. FRIT, *J. Phys. Chem. Solids* **61** (2000) 1499.
27. C. DUVERGER, M. BOUAZAOUI and S. TURELL, *J. Non. Cryst. Solids* **220** (1997) 169.
28. T. SEKIYA, N. MOCHIDA and A. SOEJIMA, *J. Non. Cryst. Solids* **191** (1995) 115.
29. T. SEKIYA, N. MOCHIDA, A. OHTSUKA and M. TONOKAUA, *J. Non. Cryst. Solids* **191** (1995) 128.
30. Y. DIMITRIEV, J. C. J. BART, V. DIMITROV and M. ARNAUDOV, *Z. Anorg. Allg. Chem.* **479** (1981) 229.
31. M. E. LINES, *J. Non. Cryst. Solids* **89** (1987) 143.

32. M. E. LINES, A. E. MILLER, K. NASSAU and K. B. LYONS, *J. Non. Cryst. Solids* **89** (1987) 163.
33. A. E. MILLER, K. NASSAU, K. B. LYONS and M. E. LINES, *J. Non. Cryst. Solids* **99** (1988) 289.
34. B. V. R. CHOWDARI and P. PRAMODA KUMARI, *J. Phys. Chem. Solids* **58**(3) (1997) 515.
35. I. V. KITYK and B. SHARAOUI, *Phys. Rev* **B60** (1999) 942.
36. G. E. KHALIL, G. A. ABDEL FATTAH, M. SALAH SHAFIK and Y. BADR, "3rd workshop on photonics and its applicatrions", IEEE, Cairo,5 Jan.(2002), IEEE Catalog No:01EX 509.

Received 21 November 2004
and accepted 12 January 2005